HHS Public Access

Author manuscript

Clin Cancer Res. Author manuscript; available in PMC 2017 June 01.

Published in final edited form as:

Clin Cancer Res. 2016 June 1; 22(11): 2778–2790. doi:10.1158/1078-0432.CCR-15-0858.

B7-H4(B7x)-mediated cross-talk between glioma initiating cells and macrophages via the IL-6/JAK/STAT3 pathway lead to poor prognosis in glioma patients

Yu Yao[#1,2], **Hongxing Ye**[#3], **Zengxin Qi**[#4], **Lianjie Mo**[#5], **Qi Yue**[4], **Aparajita Baral**[6], **Dave S.B. Hoon**[7], **Juan Carlos Vera**[8], **John D. Heiss**[8], **Clark C. Chen**[9], **Jianmin Zhang**[10], **Kunlin Jin**[11], **Ying Wang**[12], **Xingxing Zang**[13,*], **Ying Mao**[1,2,14,*], and **Liangfu Zhou**[1,2]

[1] Department of Neurosurgery, Huashan Hospital, Fudan University, Shanghai 200040, China

[2] Department of Neurosurgery, Shanghai Medical College, Fudan University, Shanghai 200032, China

[3] Department of Neurosurgery, The First Affiliated Hospital, School of Medicine, Zhejiang University, Hangzhou, Zhejiang 310003, P.R China

[4] Shanghai Medical College, Fudan University, Shanghai 200032, China

[5]Department of Neurosurgery, Sir Run Run Shaw Hospital, School of Medicine, Zhejiang University, Hangzhou 310016, China.

[6] Department of Neurosurgery, Zhongnan Hospital of Wuhan University, Wuhan, Hubei 437001, China

[7] Dept Molecular Oncology, John Wayne Cancer Institute, Santa Monica, Ca 90404, USA.

[8] Surgical Neurology Branch, National Institute of Neurological Disorders and Stroke, National Institutes of Health, 10 Center Drive, 10/3D20, MSC-1414, Bethesda, Maryland 20892-1414, USA.

[9] Center for Theoretic and Applied Oncology, University of California, San Diego, CA 92093, USA

[10] School of Medicine, Zhejiang University, Hangzhou, Zhejiang 310009, P.R China

[11] Department of Pharmacology, University of North Texas Health Science Center, Fort Worth, TX76107, USA

[12] Department of Neuropathology, Huashan Hospital, Fudan University, Shanghai 200040, China

[13]Department of Microbiology and Immunology, Albert Einstein College of Medicine, NY 10461, USA

[*] Correspondence should be addressed to Y.M (; Email: maoying@fudan.edu.cn) or X.Z. (; Email: xing-xing.zang@einstein.yu.edu)

Disclosure of Potential Conflicts of Interest: No potential conflicts of interest were disclosed.

Author contributions: Y.M., Y.Y. and X. Z. supervised the study and were responsible for manuscript preparation. Y.Y., DSBH, J.C.V., X.Z. and C.C.C. contributed to experimental design, data analyses, and the writing of the manuscript. H.X.Y., Q.Z.X, L.J.M., Q.Y., A.B. and Y.Y. performed all described experiments, except those noted below. L.F.Z. supervised the clinical specimen and contributed to manuscript revision. K.L.J. contributed to confocal microscopy dataset. Y.W. contributed the dataset related to pathologic specimen. All authors reviewed the results and commented on the manuscript.

[14] State Key Laboratory of Medical Neurobiology, School of Basic Medical Sciences and Institutes of Brain Science, Fudan University, Shanghai 200032, China.

[#] These authors contributed equally to this work.

Abstract

Purpose—The objective of this study was to evaluate clinical significance and immunosuppressive mechanisms of B7-H4 (B7x/B7S1), a B7 family member, in glioma.

Experimental Design—B7-H4 levels in glioma tissue/cerebral spinal fluid (CSF) were compared between different grades of glioma patients. Survival data were analyzed with Kaplan–Meier to determine prognostic value of B7-H4. Cytokines from CD133+ cells to stimulate the expression of B7-H4 on human Mϕs were investigated by FACS, neutralizing antibodies and transwell chemotaxis assay. shRNA, reporter vector and ChIP were used to determine the binding of STAT3 to the B7-H4 promoter. The function of B7-H4+ Mϕs in vitro was evaluated through phagocytosis, T cell proliferation/apoptosis and cytokine production as well as in xenografted model for in vivo analysis.

Results—We found that B7-H4 expression in tumors was associated with prognosis of human glioblastoma and correlated directly with malignant grades. Mechanistically, glioma initiating CD133+ cells and macrophages/microglia co-interaction activated expression of B7-H4 via IL-6 and IL-10 in both tumor cells and microenvironment supporting cells. IL-6-activated STAT3 bound to the promoter of B7-H4 gene and enhanced B7-H4 expression. Furthermore, CD133+ cells mediated immunosuppression through B7-H4 expression on macrophages/microglia by silencing of B7-H4 expression on these cells which led to increased microenvironment T cell function and tumor regression in the xenograft glioma mouse model.

Conclusion—We have identified B7-H4 activation on macrophages/microglia in the microenvironment of gliomas as an important immunosuppressive event blocking effective T-cell immune responses.

Keywords

B7-H4; glioma; immunosuppression; microglia/microphage

Introduction

Glioblastoma (GBM, WHO Grade IV) is the most aggressive and frequent *de novo* intracranial neoplasm in adults, with less than half of patients surviving longer than a year after initial diagnosis. As views changed, more emphasis was placed on the tumor-induced immunosuppression as an important factor of the formation and development of the tumor. Immunosuppressive factors secreted by both tumor cells and microenvironment T cell infiltrates are proposed to obstruct anti-tumor immunity ([1], [2]). Our hypothesis is that the tumor microenvironment cellular interactions between glioma-infiltrating macrophages/microglia (GIMs) and glioma cells play a central role in synergistically promoting glioma malignancy and immunosuppression. It has been suggested that tumor-infiltrating macrophages/microglia (TIMs) may contribute to the suppression of T-cell mediated immunity ([2], [3]). Although some secreted factors ([1], [4], [5]) and co-inhibitory immune

molecules ([4], [5]) have been reported to contribute to the immune regulation in GBM, however, the precise molecular mechanisms underlying these pathways and cellular interaction within the GBM microenvironment are poorly understood.

B7-H4 (also called B7x or B7S1) is a member of the T cell costimulatory and coinhibitory B7 family ([6-8]). Functionally, B7-H4 transmits negative signals to T cells to effectively inhibit activation, proliferation and clonal expansion of $CD4^+$ and $CD8^+$ T cells ([6-8]). Elevated expression of B7-H4 is detected in human cancer tissues of multiple cancers ([9], [10]) and is often associated with poor prognosis. We have recently determined the crystal structure of human B7x IgV functional domain and further developed a new cancer immunotherapy with mAbs targeting the B7x IgV ([11]). Previously, we reported that B7-H4 can be expressed by malignant gliomas ([12]), but its clinical significance and immunological role remain elusive. In addition, soluble B7-H4 (sB7-H4) is detected in blood from patients with ovarian, renal cell cancer, hepatocellular carcinoma, osteosarcoma, bladder urothelial carcinoma and gastric cancer ([13-18]). However, the relationship between sB7-H4 and malignant grades is still unclear. We have suspected that B7-H4 is related to a subset of tumor initiating cells in gliomas ([12]) , but details underpinning these observations remain unknown. The evolving understanding of glioma initiating cells and their importance in tumor pathophysiology ([19-25]) encourages us to consider that the interplay between glioma initiating cells and other cell types (e.g. TIMs) may be important for tumor initiation and progression in GBM.

We demonstrated Mϕs modulating cytokine production via the JAK/STAT3 pathway. B7-H4+ GIMs showed immunosuppressive activity and auto-regulation by IL-6 production. Also it was observed that adoptive immune therapy of tumor associated antigen (TAA)-specific T cells in conjunction with TIMs depleted of B7-H4 expression was able to induce tumor regression and prolonged survival of mice in xenograft human gliomas. These results revealed that circumventing the tumor-induced immunosuppression of B7-H4 can induce glioma regression. Overall our finding indicated B7-H4 as a potential immunity-associated marker of GBM, suggesting that new cancer immunotherapy targeting the B7-H4 pathway holds promise for glioma patients.

Materials and Methods

Preparation of CD133+ glioma cells

To isolate human CD133+ glioma cells, fresh primary GBM surgical specimens were dissociated mechanically and digested with a type IV collagenase (Sigma) for 1hr at 37°C. A single-cell suspension was then collected on a 30%/70% Percoll gradient and further purified by magnetic separation using anti-CD133 microbeads per the manufacturer's instructions (Miltenyi Biotec), CD133− cells were also obtained at the same time and cultured at conditions appropriate for growth (continued in Supplemental Methods).

mAb sandwich ELISA detection for sB7-H4, IL-6 and IL-10

Purified, unlabeled B7-H4-specific mAb (Clone MIH43, 2μgml^{-1}, AbDserotec) was used for coating and capture using a standard sandwich ELISA method. Thoroughly

homogenized tumor tissues were analyzed by IL-6 and IL-10 ELISA kits (eBioscience). Purified samples were then spotted in duplicate to appropriately coated plates before horseradish peroxidase-conjugated detection antibodies were added. Tetramethylbenzidine was used as a substrate for color development. The optical density was analyzed at 450 nm with a microplate reader (Spectra Max 190, Molecular Devices) and concentrations were quantified using SoftMax Pro software (Molecular Devices).

FlowCytomix Detection

Cytokine concentrations in serum, CSF and supernatant of CD133+ and CD133− cells were measured using FlowCytomix multiple kits according to the manufacturer's directions (eBioscience). Serum was obtained from fresh blood after centrifugation at 3000rpm. The supernatant was collected after culture for 72hr and stored at −20°C. For FlowCytomix detection, the supernatant was added in duplicate to coated 96-well plates. After fluorescent polystyrol beads were coupled with antibodies specific to the cytokines, biotins and streptavidin-PE were successively added. After being activated (690nm), samples were analyzed by flow cytometry and quantified with FlowCytomix Pro 2.4 software. Detected cytokines included: MIP-1α, MCP-1, MIP-1β, IL-8, RANTES, MIG, IL-6, IL-10, GM-CSF, and IL-4.

Flow cytometry

To detect surface B7-H4, CD11b or CD133 expression, cells were incubated on ice for 30min with appropriate antibodies or isotype controls (PE-B7-H4, PE-mouse IgG1, APC-CD11b, APC-CD133, APC-mouse IgG1, all from eBioscience, 1:5), washed twice with FACS buffer (PBS containing 0.1% NaN3 and 5% fetal bovine serum), and resuspended in 0.5 ml 1% formalin/PBS. To analyze intracellular B7-H4, cells were pre-treated with Fix and Perm cell permeabilization reagents (Caltag Laboratories) according to the manufacturer's instructions. Assays of immune function, cell proliferation, cell cycle, apoptosis, cytokines and cytotoxicity were done under standard methods as previously described. All analyses were performed on a FACS calibur system (Becton Dickinson Immunocytometry Systems).

qRT-PCR

Total RNA from cells was isolated using an RNA purification kit (Qiagen) and treated with RNase-free DNase I to remove genomic DNA (Roche). cDNA libraries were generated using Superscript RNase H-Reverse Transcriptase (Invitrogen) and random hexamers (Sigma-Aldrich). qRT-PCR was performed in an ABI Prism7500 sequence detection system (Applied Biosystems) with SYBR Green Master Mix (Eurogentec) and primers (Sangon Biotech Co. Ltd) at optimized concentrations. Primer sequences for B7-H4 were 5'-TCTGGGCATCCCAAGTTGAC-3' (forward primer) and 5'-TCCGCCTTTTGATCTCCGATT-3' (reverse primer), housekeeping GAPDH primers have been described previously. Standard curves were obtained for each gene and the amplification was 90% to 100% efficient. All values were normalized to GAPDH and relative RNA expression was determined and compared to control groups.

Regulation of B7-H4 expression

To regulate B7-H4 expression, Mϕs or microglia were cultured for 72hr with CD133+ cells or CD133− cells at the ratio of 10:1, CD133+ supernatant or CD133− supernatant or different concentrations of recombinant IL-10, IL-6, IL-4, and GM-CSF (Peprotech). Neutralizing monoclonal antibodies against human IL-6 (anti–IL-6, clone 6708, 500 ng/ml^{-1}) and IL-10 (anti–IL-10, clone 23738, 50 ngml^{-1}) (Peprotech) were used as indicated. For B7-H4 blocking, fresh macrophages were transfected with lentiviral two pairs of short-hairpin (sh)-B7-H4 and sh-mock as directed (Shanghai gene chemical technology limited company, China). RT-PCR and flow cytometry were performed to quantify B7-H4 mRNA and surface protein expression.

In vitro TAA-specific T cell immunosuppression

Dendritic cells (DCs) extracted from peripheral blood mononuclear cells (PBMCs) or mouse bone marrow by CD11c microbeads (Miltenyi Biotec) were incubated with irradiated apoptotic U87MG or GL261 cells at a ratio of 1:5 for 24h. These tumor-loaded DCs (2×10^4 cellswell^{-1}) were then used to activate CD3+ T-cells from blood or CD8+ T cells from spleen (2×10^5 cellswell^{-1}) in the presence of 10 Uml^{-1} IL-2 and 10 ngml^{-1} IL-7 for 1wk. To evaluate proliferation, cell cycle stage, apoptosis or cytokine secretion, TAA-specific T cells were cocultured with different macrophages at a 1:1 ratio, stained with CFSE, PI, annexin V/PI or IL-2/IFNγ, and sorted by FACS. To measure cytotoxicity, CD8+ T-cells isolated from blood was stimulated by macrophages at various ratios and cocultured with CFSE-labeled U87MG cells. FACS was performed with annexin V/PI staining and cytotoxicity was quantified as the percentage of dead or apoptotic cells. For LDH release assay, Mϕs/microglias and activated CD8+ T-cells (Mϕ/microglia:T=40:1, 20:1, 10:1, 1:1, 1:10, 1:20) were added with or without 1×10^5 GL261 cells per well. After a 12h coculture, the supernatant from each well was collected and analyzed with CytoTox 96 Non-Radioactive Cytotoxicity Assay kit (Promega Corporation) and recorded at an absorbance of 490nm.

Statistical analysis

The two-tailed Student's t-test was performed to assess the significance between experimental groups. The Pearson correlation or linear regression analysis was used for correlations between parameters. Cumulative survival time was calculated by the Kaplan-Meier method and comparison between the groups was tested by the log-rank test. GraphPad software (GraphPad Software, Inc, version 5.02) was used for all statistical analyses. Statistically significant P values are indicated in the figures with asterisks: ***, $P < 0.001$; **, $P < 0.01$; *, $P < 0.05$.

RESULTS

Elevated B7-H4 expression associated with human glioma progression

We examined the relationship between glioma B7-H4 expression and disease progression in the patients of different stages. B7-H4 mRNA levels in glioma tissues with WHO Grade I-IV and normal control brain tissue from epilepsy surgery (Non-Tumor controls) were compared. B7-H4 mRNA expression increased with higher grade tumor stage (Fig. 1A).

Furthermore, to verify these findings, the expression of B7-H4 was examined by IHC in 138 glioma and six Non-Tumor control tissues (tissue microarray: TMA, Supplementary Table 1). We observed immunoreactivity of B7-H4 protein in both the cytoplasm and membrane (Fig. 1B), and a very low level of B7-H4 expression was observed in control compared with glioma tissues. Western blot (WB) analysis showed high expression of B7-H4 protein in high-grade gliomas (HGG), minimal expression in low-grade gliomas (LGG), and negligible detection in Non-Tumor controls (Fig. 1C). Significant differences for B7-H4 staining pattern were observed between controls and LGG (P<0.001) and between LGG (n=33) and HGG (n=105) (P <0.001, Fig. 1D). We searched the Cancer Genome Atlas (TCGA) data GBM gene expression profile for expression of B7-H4. Compared with normal brain tissue (n=10), B7-H4 overexpressed in GBM tissue (n=483). We futher analysed the gene expression correlated with GBM phenotype, and found that B7-H4 gene up-regulation mainly exists in proneural type (**Supplementary Figure 1**).

Flow cytometry was used to assess glioma tissues, B7-H4+CD11b+ Mϕs/microglia in LGG and HGG were 24.5% and 69.9% (Fig. 1E, P <0.01), respectively. We also assessed B7-H4 in peripheral blood cells (n=8/healthy group, 13/LGG group, 10/HGG group) and glioma specimens (n=8/LGG group, 8/HGG group) was characterized. In blood, B7-H4+CD11b+ monocytes in LGG and HGG were 8.5% and 14.4%, (Fig. 1E, P>0.05), respectively.

Prior studies demonstrated a correlative relationship between sB7-H4 and severity of ovarian cancer and renal cancer ([13], [14]), however the role of sB7-H4 in human glioma is unclear. We used ELISA to detect sB7-H4 in CSF from 52 patients (clinical characteristics of patients on Supplementary Table 1). We found that increasing concentrations of sB7-H4 in CSF was associated with higher malignancy stages (Fig. 1F). This analysis demonstrated sB7-H4 is released into the CSF of glioma patients and associated with advanced stages in the disease.

Retrospective analysis of B7-H4 expression in GBM to correlate with survival

A large cohort of GBM patients tumors (n=70, Supplementary Table 2) was retrospectively analyzed for B7-H4 expression by IHC to determine prognostic value. We identified an inverse correlation of tumor cell B7-H4 expression levels (negative vs moderate vs. strong) and survival in terms of progression-free survival (PFS) and overall survival (OS) (Fig. 1G. PFS: P<0.001,OS: P<0.001). This findings suggested a role for B7-H4 as a potential predictor of poor disease outcome.

B7-H4 distribution in both GIMs and tumor cells in glioma tissues

A murine glioma model in C57BL/6 mice was developed to further examine B7-H4 in tumors and GIMs (CD11b+/CD45+Mϕs). Higher levels of B7-H4 expression were found in GL261-derived intracranial tumors (Fig. 2A-B). B7-H4+ GIMs (Iba1+ Mϕs) were identified primarily at the glioma tumor boundary. (Fig.2C, 88.3% for boundary vs 38.8% for intratumoral, ***P<0.001). We isolated GIM by CD11b magnetic microbeads from the mouse glioma tumor tissues. GIM were further identified in their role in GBM surveillance ([26], [27]) and found that the isolated cell population of GIMs expressed higher levels of surface B7-H4:74±1% for GIMs vs 15±7% for Mϕs/microglia from controls (Fig. 2D, E,

P<0.001). We compared levels of B7-H4 expression in GL261 cells cultured *in vitro* with GL261 cells implanted into mice and revealed a lower capacity for induction of B7-H4 expression in in-vitro cultured GL261 cells, 2±1.6% versus 6±2%, p <0.05 (Fig. 2F**).** To confirm this, GL261 cells from model mouse were isolated and analyzed by Western blot from vitro cultured GL261 cells as controls. Isolated GIMs from xenografts expressed higher levels of B7-H4 from Non-Tumor controls. (Supplementary Figure 2)

Clinical tumors were assessed to determine if the murine tumor observation also show a similar response. MRI and magnetic resonance spectroscopy (MRS) were used to characterize patient intracranial gliomas. For these studies, peritumoral (stromal) and tumor-nest regions were identified (Fig. 2G). Enhanced MRI images-guided brain tissue biopsies taken from these locations were sectioned to include both regions of interest and then employed IHC with anti-B7-H4, cell-specific, anti-Iba1, and anti-CD8 Abs for GIMs (Mϕs/microglia) and CTLs, respectively. The IHC analysis revealed higher amounts of B7-H4 on GIMs in the peritumoral regions (Fig. 2G). Immunofluorescence (IF) for GBM tissues proved that not only GIMs but also CD133+ tumor cells expressed B7-H4 as previously shown (Fig. 2H) ([12]).

Together our results confirmed the presence of both cellular and soluble forms of B7-H4 and established GIMs and glioma cells (including CD133+ cells) as candidates for the sources of this protein. Considering their important role, we further explored the cross-talk between GBM CD133+ cells and GIMs in the glioma microenvironment.

CD133+ cells produce IL-6 and IL-10 to activate B7-H4 expression on Mϕs

We next examined whether GBM CD133+ cells could regulate B7-H4 expression in Mϕs. Fresh normal Mϕs were incubated in specific culture conditions: control medium only, medium and CD133+ GBM cells, medium and CD133− GBM cells, and supernatant of CD133+ or CD133− cells. After 72hrs of incubation, B7-H4 expression on Mϕs was assessed by flow cytometry. Mϕs co-cultured with CD133+ cells expressed higher B7-H4 than those cultured devoid of CD133+ cells (56.1% for CD133+ cell co-culture vs 28.8% for CD133− cell co-culture, *P* <0.05, Fig.3A). Mϕs exposed to CD133+ cell supernatant also had higher B7-H4 expression than those exposed to CD133− cell supernatant (49.3% for CD133+ supernatant vs 16.6% for CD133− supernatant, *P*<0.01, Fig. 3A). These findings were supported by RT-qPCR studies of B7-H4 expression of Mϕs in CD133+ and CD133− supernatant (Fig. 3B) in which marked significant elevation of B7-H4 expression was most notable in Mϕs cultured in CD133+ supernatant.

We hypothesized that factors secreted by CD133+ cells had a major role in up-regulating B7-H4 expression. To test this, FlowCytomix was used to establish cytokine profiles for CD133+ and CD133− supernatant. Two significant chemokines, MIP-1α and MCP-1, were found to be at substantially higher concentrations in CD133+ supernatant relative to CD133− supernatant (Fig. 3C, P<0.001). Interestingly, levels of IL-6 and IL-10 were also elevated in CD133+ media relative to CD133− supernatant (*P*<0.001, Fig.3C). To determine their roles, IL-6 and IL-10 were added to control cultures of Mϕs. We observed a dose-dependent up-regulation of B7-H4 expression in Mϕs stimulated by these cytokines (Fig.

3D) and verified these findings by suppressing an IL-6 and IL-10 activity with specific Ab, respectively (Fig. 3E).

Because these results suggested a primary role of interleukins IL-6 and IL-10 in regulating B7-H4 expression that occurs in the microenvironment, we further investigated systemic levels of these cytokines. FlowCytomix was performed with serum and CSF from a series of glioma patients (clinical characteristics in Supplementary Table 1). Only trace amounts of these cytokines were detected in serum and CSF. A relationship between the serological interleukin levels and tumor grade was not readily delineated, ELISA analysis from tissue homogenates identified elevation of these two cytokines, and showed a higher level of IL-6 in HGG patients ($P<0.01$) compared to control patients (Supplementary Fig. 3). This finding supports a role for these two cytokines in GBM and induction of immunosuppression, perhaps more confined to the tumor microenvironment than system-wide. Finally, we used a cell migration assays to examine if CD133+ GBM cells could initiate recruitment of Mϕs/monocytes into the tumor environment. We found enhanced migration of Mϕs/monocytes with CD133+supernatant as a chemo-attractant (Fig. 3F, medium-only, CD133+ and CD133− supernatant: 1±0.00, 5.17±0.78 and 3.12±0.22 respectively).

These findings support a novel mechanism by which CD133+ cells are able to induce Mϕs migration into the tumor microenvironment and induce them to express B7-H4 by cytokines IL-6 and IL-10.

IL-6 induces B7-H4 expression via the JAK/STAT3 pathway

Considering that enhanced IL-6 was found in glioma tissue homogenates (Supplementary Fig.3), we then explored the molecular pathways through which B7-H4 expression was regulated. IL-6 signaling has been extensively investigated through the JAK/STAT pathway([28]), so we hypothesized that the expression of B7-H4 was regulated through this pathway. To confirm this, mouse BV2 microglia cells were stimulated with IL-6 and analyzed the phosphorylation of STAT3 by Western blot. As shown in Fig.4A, IL-6 treatment up-regulated phosphorylation of Stat3 and B7-H4 levels in BV2 cells in a dose and gradient dependent manner, and 25 ng/ml and 24 hr were suitable dosage and time point. Similar findings were reproduced in the mouse RAW Mϕs cell line (Fig.4B) and Mϕs sorted from healthy human peripheral blood (Fig.4C).

To further determine whether the expression of B7-H4 was regulated by the Stat3 pathway, four pairs of STAT3 shRNAs were individually transduced into BV2 cells to knock down endogenous STAT3. STAT3 mRNA in BV2 cells transduced with lentiviral stocks expressing shRNA1, shRNA2, shRNA3, or shRNA4 were reduced by 54.2, 65.0, 85.3, and 78.6%, respectively (Fig.4D left). Because STAT3 protein was remarkably decreased in the BV2 cells that were transduced with shRNA3, we chose to use shRNA3 for the subsequent experiments. We found that silencing STAT3 with shRNA3 reduced B7-H4 expression with or without the stimulation of IL-6 (Fig. 4E). WB analysis of BV2 microglia stimulated with CD133+ supernatant was also performed, which showed similar tendency as IL-6 did (Supplementary Fig.4).

We next determined whether STAT3 could be a transcriptional regulator of the B7-H4 gene. We transfected BV2 microglia cells with a reporter vector encoding Luciferase under control of the B7-H4 promoter (PGL3-B7H4.WT). Phosphorylation of STAT3 up-regulated B7-H4 promoter activity, which was abrogated by knockdown of STAT3 with shRNA (Fig.4F). These studies suggested that STAT3 regulated B7-H4 transcription via enhancing the B7-H4 promoter. We then carried out chromatin immunoprecipitation (ChIP) assays to assess whether STAT3 directly binds to the B7-H4 promoter. As shown in Fig. 4G, STAT3 protein bound to the B7-H4 promoter was significantly increased in BV2 microglia cells treated with IL-6. The epistatic relationship between the expression of B7-H4 and IL-6—STAT3 pathway (Supplementary Fig.5), may provide a new line of evidence for the development of STAT3 inhibitor as anti-cancer chemotherapy drugs.

CD133+ cells mediate immunosuppression through B7-H4+ Mφs *in vitro* and *in vivo*

In order to explore the role of B7-H4 in CD133+ cell-mediated immunosuppression, CD133+ cells were sorted from human GBM cell suspensions, and the supernatant of CD133+ cell culture was then used to treat normal Mφs to induce expression of B7-H4. We found that CD133+ cell supernatant-treated Mφs showed markedly reduced uptake of red fluorescent tag labeled polystyrene latex beads compared with CD133− cell supernatant-treated Mφs (Fig. 5A), suggesting that the supernatant of CD133+ cells inhibits the phagocytotic activity of Mφs. We then examined the function of B7-H4 in Mφs induced by the supernatant of CD133+ cells. B7-H4 expression in Mφs was silenced by shRNA (Fig. 5B) and Mφs were co-cultured with T cells activated by U87MG-loaded CD11c+ DCs. We found that the B7-H4 silencing in Mφs increased T cell proliferation (Fig. 5C) and decreased T cell apoptosis (Fig. 5D). Correspondingly, the B7-H4 silencing also reduced T cells that did not produce IL-2 or IFN-γ (Fig. 5E). Furthermore, B7-H4+ Mφs cultured in CD133+ supernatant inhibited CTL-cytotoxic activity against U87MG glioma cells. However, the inhibitory effects were mitigated after B7-H4 expression was blocked (Fig.5F).

To investigate the function of B7-H4 in Mφs *in vivo*, we utilized the GL261-induced glioma mouse model. GL261 tumor cells derived from mouse glioma contained CD133+ cells and were able to inhibit both CD8+ and CD4+ T cell function in vitro (Supplementary Fig. 6). Interestingly, the suppressive capacities were partially reversed by exposing Mφs to anti-B7-H4 ab (Supplementary Fig. 6). These results suggested that CD133+ cells can induce B7-H4 expression on Mφs, which leads to T cell inhibition.

Suppression of B7-H4 leads to T-cell activation and tumor regression in the xenograft glioma model

NOD/SCID xenograft gliomas derived from U87MG cells were further investigated. TAA-specific CD8+ T cells (CTL) were injected intravenously together with: 1) normal Mφs (M), 2) CD133+ Glioma initiating cells conditioned Mφs (GCM), 3) conditioned Mφs transduced with sh1-mock, or 4) conditioned Mφs transduced with sh1-B7-H4 to silence B7-H4 expression. We observed tumor growth inhibition in mice injected together with CTL+ M and CTL+ GCM+ sh1-B7-H4 Mφs, while the other two groups showed rapid progression of nearly 200 mm^3 per day (Fig. 5G, 5H). These results suggested that CD133+ cells played a primary role in driving B7-H4+ Mφs to reduce TAA-specific T cell immunity *in vivo*.

To determine whether B7-H4 could serve as a predictor of prognosis, we infused CTLs with CD133+ Glioma initiating cells-conditioned sh1-mock or sh-B7-H4 Mϕs via a caudal vein injection of mice with U87MG-derived intracranial tumor. Mice with sh1-B7-H4 treated Mϕs survived significantly longer than the sh1-mock group (Fig. 5I). In contrast, mice infused with PBS and sh1-mock treated Mϕs had U87MG cell invasion, which was also characterized by early lesions detected by MRI (Fig. 5J). Supporting the role of Mϕs in regulating T cell function, human CD11b+ Mϕs/microglia and human CD8+ T cells appeared to co-migrate into intracranial human tumors (Fig. 5K).

GIMs induce B7-H4 expression in CD133+ cells and auto-regulation through IL-6

GIMs were isolated from murine GL261 tumors to investigate their effects on CD133+ cells. Using a transwell chemotaxis assay in a co-culture system, migration abilities between GIMs and normal Mϕs/microglia (NMs) were compared. GIMs exhibited higher time-dependent migration abilities (Fig. 6A).

Next, GL261-derived enriched CD133+ cells were separated from CD133− cells, and both cell populations were cultured in GIM-conditioned media. GIMs up-regulated B7-H4 expression in CD133+ cells and CD133− cells according to flow cytometry, IF and WB analysis (Fig. 6B-D). Considering IL-6 and IL-10 were involved in B7-H4 induction, we measured the level of these cytokines in the sera of: 1) normal mice, 2) CD133− cells initiated tumor mice, 3) CD133+ cells initiated tumor group, and supernatants groups from NM and GIM cultures. There was no observable difference in serum IL-6 levels across the three groups. However, we observed that GIM-secreted IL-6 exceeded NM-secreted IL-6 by >15 folds (Fig. 6E). No difference was observed for IL-10 concentrations in these groups (data not shown). These results support a role for IL-6 promoting B7-H4 expression in the tumor microenvironement. Finally, we also find IL-6 can up-regulate B7-H4 expression in mice NMs *in vitro as* human Mϕs did (data not shown). The results showed that Mϕs/microglia in the tumor environment had markedly-enhanced B7-H4 expression in the presence of CD133+ Glioma initiating cells.

DISCUSSION

Immunosuppressive processes occurring both systemically and locally in the tumor microenvironment have limited the normal function of the immune system in primary brain malignancies. Our studies characterizing the immunological roles of GIMs, tumor derived cytokines, and tissue-derived Glioma initiating cells have revealed evidence for an immunosuppressive role of B7-H4 in human malignant glioma.

We found that increasing B7-H4 expression associated with progression of human glioma. Notably, the distribution of B7-H4 expressing cells was much higher at the peritumoral edges (i.e. stroma) when compared to the tumor nest. What was important, our studies demonstrated that PFS and OS is negatively correlated with expression of B7-H4 in human gliomas. Expression of B7-H4 was detected on the surface of CD11b+/Iba+ monocytes, microglia, and macrophages. CD8+ T cells have been shown to orchestrate autoimmunity in immune privileged locations ([29]) and anti-tumor immunity in malignancy ([30], [31]). Interestingly, we found that CD8+ T cells were also mainly present at the peritumoral edges.

Co-localization of B7-H4, Mϕs/microglia, and CD8+ T cells at peritumoral edges suggests a functional connection in the tumor microenvironment on the periphery but not internally. We found significantly higher levels of IL-6 in HGG group compared to LGG or LGG group compared to the normal, but not in serum, suggesting that the immunosuppressive effects of the cytokines are limited to the tumor environment.

B7-H4 in the tumor microenvironment, surrounding stroma and invasive edge, may contribute to the escape from immune surveillance during tumor cell invasion into adjacent brain tissue. We believe that recruitment of monocytes/Mϕs to the tumor at the glioma site occurs in the malignant state ([32], [33]). The development of these TIMs is stimulated by "polarization" induced by the glioma and other tumor cells, resulting in TIMs with a tumor-promoting phenotype (M2). A chemokine-mediated process that spawns tumor development in the microenvironment is demonstrated ([27], [34], [35]). It is also demonstrated that microglia derived from non-glioma human subjects could curb glioma cell growth by the secretion of chemokine like IL-8 and MCP-1, but microglia and monocytes cultured from glioma patients were inefficient at reducing the sphere-forming capacity of tumor cells([36]). Our studies showed Glioma initiating cells mediated expression of B7-H4 on Mϕs. Moreover, the detection of Mϕ-recruiting chemokines, MIP-1α and MCP-1, which are secreted by CD133+ Glioma initiating cells presents evidence to support a process whereby Mϕs are signaled to invade the tumor microenvironment.

Our experimental findings demonstrated that normal monocytes/Mϕs were induced to express B7-H4 via IL-6 and IL-10 by human $CD133^+$ cells (Fig.3) or U251 glioma initiating cells (our published data([37])). In turn, a suppressive potential conferred by Mϕs expressing B7-H4 contributed to immunopathology based on several lines of evidence. First, forcing B7-H4 expression on Glioma initiating cells impaired phagocytosis in normal Mϕs, inhibited T cell proliferation and cytokine production, and led to reduced cytotoxicity of T cells. Second, blocking B7-H4 expression significantly impaired the Mϕs' suppressive capacity. Third, despite the presence of potent TAA-specific effector T cells *in vivo*, CD133+ cell-conditioned Mϕs promoted intracranial and subcutaneous tumor growth in SCID/NOD mice bearing human gliomas. Co-localization of human CTL and Mϕs/microglia *in vivo* in our mouse model presents new evidence for the role of B7-H4+ GIMs in immunomodulatory function.

Antitumor effects appear to be obstructed by a dichotomous mechanism that eliminates M1 macrophage-mediated innate immune responses and impairs T cell activation. We observed that CD133+ cells stimulated by GIMs, which secreted high levels of IL-6, expressed B7-H4 but did not secrete notable amounts of IL-6 or IL-10 into sera. Functionally, IL-6 resulted in B7-H4 expression in Mϕs. Other studies also demonstrated that IFN-γcould upregulate B7-H4 expression on mouse embryo fibroblasts, but detailed pathway was unknown ([38]). It seems plausible that Glioma initiating cells native to the tumor microenvironment trigger immunosuppression in part by "recruiting and talking" to Mϕs. Following an initial exchange with the GSGs, the Mϕs became polarized to the M2 type and integrated into an external role in the developmental stage of this immunomodulatory process and conducted persistent "B7-H4 education" through auto-regulation. This intimate process is further promoted by Glioma initiating cells and fosters the immunosuppressive conditions mounted

in the tumor stroma. The immunosuppressive association between Glioma initiating cells and GIMs may thus be defined in the context of time (early vs. late) and space (niche-inhabiting vs. recruitment and marginalization) to explain the proposed role of B7-H4 as a potential immunity-associated marker for malignancy progression and prognosis (Supplementary Figure 7).

In this study we showed that CSF sB7-H4 concentration tended to correlate with malignancy grades of glioma. The blood-brain barrier (BBB) normally allows the permeability of small molecules (400–500 Da) and some small lipid-soluble proteins([39]), B7-H4 (50 kDa - 80 kDa) may be too large to pass across this natural barrier. Considering CSF comes in direct contact with the extracellular compartment of the central nervous system and the existence of BBB, CSF sB7-H4 may be a better potential immunity-associated marker for supratentorial tumors like gliomas when compared to serum sB7-H4. Enrolling more research subjects with intracranial immunological diseases to reflect the enhanced utility of sB7-H4 in CSF over sB7-H4 from serum may be needed.

In summary, our studies demonstrated a direct relationship between WHO grading of gliomas and the levels of B7-H4, suggesting its utility as a potential immunity-associated marker for progression of the disease. We established crucial roles of B7-H4 in the cellular interplay of glioma-mediated immunosuppression between CD133+ Glioma initiating cells and TIMs/GIMs, and uncovered that such a “cross talking” contributed to glioma pathology. This study revealed a previously unrecognized immune evasion route and provided an anti-B7-H4 therapeutic target in patients with malignant gliomas.

Supplementary Material

Refer to Web version on PubMed Central for supplementary material.

Acknowledgements

We thank Jian Hu (MD Anderson Cancer Center) , Daniel A. Tennant (University of Birmingham) for helpful advice, Xin Zhang (Fudan University) for assistance with patients follow-up, and Ran Tao (Shanghai Jiaotong University) for helpful discussions.

Grant Support: This work was supported by the National Science Foundation for Distinguished Young Scholars of China (Grant No. 81025013 to Y.M), the National Natural Science Foundation of China (Grant No. 81372708, 81272797 to Y.Y.), the Project for National 985 Engineering of China (No.985 III-YFX0102 to Y.M), the “Dawn Tracking” Program of Shanghai Education Commission, and China Grant 10GG01 (to Y. M),the Project for Science and Technology Commission of Shanghai Municipality Grant 13JC1408000 (to L.F.Z), innovation Program of Shanghai Municipal Education Commission (Grant No. 13ZZ010 to Y.Y.).

References

1. Fong B, Jin R, Wang X, Safaee M, Lisiero DN, Yang I, et al. Monitoring of regulatory T cell frequencies and expression of CTLA-4 on T cells, before and after DC vaccination, can predict survival in GBM patients. PLoS One. 2012; 7:e32614. [PubMed: 22485134]
2. Rolle CE, Sengupta S, Lesniak MS. Mechanisms of immune evasion by gliomas. Adv Exp Med Biol. 2012; 746:53–76. [PubMed: 22639159]
3. Zhai H, Heppner FL, Tsirka SE. Microglia/macrophages promote glioma progression. Glia. 2011; 59:472–85. [PubMed: 21264953]

4. Parsa AT, Waldron JS, Panner A, Crane CA, Parney IF, Barry JJ, et al. Loss of tumor suppressor PTEN function increases B7-H1 expression and immunoresistance in glioma. Nat Med. 2007; 13:84–8. [PubMed: 17159987]
5. Yao Y, Tao R, Wang X, Wang Y, Mao Y, Zhou LF. B7-H1 is correlated with malignancy-grade gliomas but is not expressed exclusively on tumor stem-like cells. Neuro Oncol. 2009; 11:757–66. [PubMed: 19264916]
6. Zang X, Loke P, Kim J, Murphy K, Waitz R, Allison JP. B7x: a widely expressed B7 family member that inhibits T cell activation. Proc Natl Acad Sci U S A. 2003; 100:10388–92. [PubMed: 12920180]
7. Prasad DV, Richards S, Mai XM, Dong C. B7S1, a novel B7 family member that negatively regulates T cell activation. Immunity. 2003; 18:863–73. [PubMed: 12818166]
8. Sica GL, Choi IH, Zhu G, Tamada K, Wang SD, Tamura H, et al. B7-H4, a molecule of the B7 family, negatively regulates T cell immunity. Immunity. 2003; 18:849–61. [PubMed: 12818165]
9. Zang X, Thompson RH, Al-Ahmadie HA, Serio AM, Reuter VE, Eastham JA, et al. B7-H3 and B7x are highly expressed in human prostate cancer and associated with disease spread and poor outcome. Proc Natl Acad Sci U S A. 2007; 104:19458–63. [PubMed: 18042703]
10. Quandt D, Fiedler E, Boettcher D, Marsch W, Seliger B. B7-h4 expression in human melanoma: its association with patients' survival and antitumor immune response. Clin Cancer Res. 2011; 17:3100–11. [PubMed: 21378130]
11. Jeon H, Vigdorovich V, Garrett-Thomson SC, Janakiram M, Ramagopal UA, Abadi YM, et al. Structure and cancer immunotherapy of the B7 family member B7x. Cell Rep. 2014; 9:1089–98. [PubMed: 25437562]
12. Yao Y, Wang X, Jin K, Zhu J, Wang Y, Xiong S, et al. B7-H4 is preferentially expressed in non-dividing brain tumor cells and in a subset of brain tumor stem-like cells. J Neurooncol. 2008; 89:121–9. [PubMed: 18478183]
13. Simon I, Zhuo S, Corral L, Diamandis EP, Sarno MJ, Wolfert RL, et al. B7-h4 is a novel membrane-bound protein and a candidate serum and tissue biomarker for ovarian cancer. Cancer Res. 2006; 66:1570–5. [PubMed: 16452214]
14. Thompson RH, Zang X, Lohse CM, Leibovich BC, Slovin SF, Reuter VE, et al. Serum-soluble B7x is elevated in renal cell carcinoma patients and is associated with advanced stage. Cancer Res. 2008; 68:6054–8. [PubMed: 18676826]
15. Zhang C, Li Y, Wang Y. Diagnostic value of serum B7-H4 for hepatocellular carcinoma. J Surg Res. 2015; 197:301–6. [PubMed: 25963168]
16. Dong Q, Ma X. B7-H4 expression is associated with tumor progression and prognosis in patients with osteosarcoma. BioMed Res Int. 2015; 2015:156432. [PubMed: 25954746]
17. Liu WH, Chen YY, Zhu SX, Li YN, Xu YP, Wu XJ, et al. B7-H4 expression in bladder urothelial carcinoma and immune escape mechanisms. Oncol Lett. 2014; 8:2527–34. [PubMed: 25364421]
18. Shi H, Ji M, Wu J, Zhou Q, Li X, Li Z, et al. Serum B7-H4 expression is a significant prognostic indicator for patients with gastric cancer. World J Surg Oncol. 2014; 12:188. [PubMed: 24947047]
19. Bao S, Wu Q, McLendon RE, Hao Y, Shi Q, Hjelmeland AB, et al. Glioma stem cells promote radioresistance by preferential activation of the DNA damage response. Nature. 2006; 444:756–60. [PubMed: 17051156]
20. Chen J, Li Y, Yu TS, McKay RM, Burns DK, Kernie SG, et al. A restricted cell population propagates glioblastoma growth after chemotherapy. Nature. 2012; 488:522–6. [PubMed: 22854781]
21. Driessens G, Beck B, Caauwe A, Simons BD, Blanpain C. Defining the mode of tumour growth by clonal analysis. Nature. 2012; 488:527–30. [PubMed: 22854777]
22. Hemmati HD, Nakano I, Lazareff JA, Masterman-Smith M, Geschwind DH, Bronner-Fraser M, et al. Cancerous stem cells can arise from pediatric brain tumors. Proc Natl Acad Sci U S A. 2003; 100:15178–83. [PubMed: 14645703]
23. Nguyen LV, Vanner R, Dirks P, Eaves CJ. Cancer stem cells: an evolving concept. Nat Rev Cancer. 2012; 12:133–43. [PubMed: 22237392]

24. Schepers AG, Snippert HJ, Stange DE, van den Born M, van Es JH, van de Wetering M, et al. Lineage tracing reveals Lgr5+ stem cell activity in mouse intestinal adenomas. Science. 2012; 337:730–5. [PubMed: 22855427]
25. Singh SK, Clarke ID, Terasaki M, Bonn VE, Hawkins C, Squire J, et al. Identification of a cancer stem cell in human brain tumors. Cancer Res. 2003; 63:5821–8. [PubMed: 14522905]
26. Badie B, Schartner JM, Paul J, Bartley BA, Vorpahl J, Preston JK. Dexamethasone-induced abolition of the inflammatory response in an experimental glioma model: a flow cytometry study. J Neurosurg. 2000; 93:634–9. [PubMed: 11014542]
27. Wu A, Wei J, Kong LY, Wang Y, Priebe W, Qiao W, et al. Glioma cancer stem cells induce immunosuppressive macrophages/microglia. Neuro Oncol. 2010; 12:1113–25. [PubMed: 20667896]
28. Briscoe J, Guschin D, Rogers NC, Watling D, Muller M, Horn F, et al. JAKs, STATs and signal transduction in response to the interferons and other cytokines. Philoso Trans R Soc Lond B Biol Sci. 1996; 351:167–71.
29. Palmer DC, Chan CC, Gattinoni L, Wrzesinski C, Paulos CM, Hinrichs CS, et al. Effective tumor treatment targeting a melanoma/melanocyte-associated antigen triggers severe ocular autoimmunity. Proc Natl Acad Sci U S A. 2008; 105:8061–6. [PubMed: 18523011]
30. Appay V, Douek DC, Price DA. CD8+ T cell efficacy in vaccination and disease. Nat Med. 2008; 14:623–8. [PubMed: 18535580]
31. Klebanoff CA, Gattinoni L, Restifo NP. CD8+ T-cell memory in tumor immunology and immunotherapy. Immunol Rev. 2006; 211:214–24. [PubMed: 16824130]
32. Ginhoux F, Greter M, Leboeuf M, Nandi S, See P, Gokhan S, et al. Fate mapping analysis reveals that adult microglia derive from primitive macrophages. Science. 2010; 330:841–5. [PubMed: 20966214]
33. Pollard JW. Tumour-educated macrophages promote tumour progression and metastasis. Nat Rev Cancer. 2004; 4:71–8. [PubMed: 14708027]
34. Gabrilovich DI, Ostrand-Rosenberg S, Bronte V. Coordinated regulation of myeloid cells by tumours. Nat Rev Immunol. 2012; 12:253–68. [PubMed: 22437938]
35. Kerkar SP, Restifo NP. Cellular constituents of immune escape within the tumor microenvironment. Cancer Res. 2012; 72:3125–30. [PubMed: 22721837]
36. Sarkar S, Doring A, Zemp FJ, Silva C, Lun X, Wang X, et al. Therapeutic activation of macrophages and microglia to suppress brain tumor-initiating cells. Nat Neurosci. 2014; 17:46–55. [PubMed: 24316889]
37. Mo LJ, Ye HX, Mao Y, Yao Y, Zhang JM. B7-H4 expression is elevated in human U251 glioma stem-like cells and is inducible in monocytes cultured with U251 stem-like cell conditioned medium. Chin J Cancer. 2013; 32:653–60. [PubMed: 23327799]
38. Rahbar R, Lin A, Ghazarian M, Yau HL, Paramathas S, Lang PA, et al. B7-H4 expression by nonhematopoietic cells in the tumor microenvironment promotes antitumor immunity. Cancer Immunol Res. 2015; 3:184–95. [PubMed: 25527357]
39. Rubin LL, Staddon JM. The cell biology of the blood-brain barrier. Annu Rev Neurosci. 1999; 22:11–28. [PubMed: 10202530]

Translational Relevance

Glioblastoma (GBM) is the most malignant and lethal primary brain tumor. To understand the mechanisms underlying GBM progression is critical for clinical practice. This study revealed the complex immune interactions in the GBM tumor microenvironment involving immune checkpoint B7-H4 and IL-6 regulatory mechanisms during tumor progression. Specifically the results identified that B7-H4+ glioma infiltrated macrophages (Mϕs)/microglia showed immunosuppressive activity which could be auto-regulated by IL-6 production. IL-6-activated STAT3 bound to the promoter of B7-H4 gene and enhanced B7-H4 expression on Mϕs. Our studies demonstrated a direct relationship between the grade of gliomas and the levels of B7-H4 expression, suggesting it as a potential immune-associated marker for progression of gliomas. The findings were further demonstrated using in vivo xenografts model. Overall our study contributes to the understanding of GBM progression, and suggests that targeting the B7-H4 pathway holds therapeutic promise for advanced glioma patients.

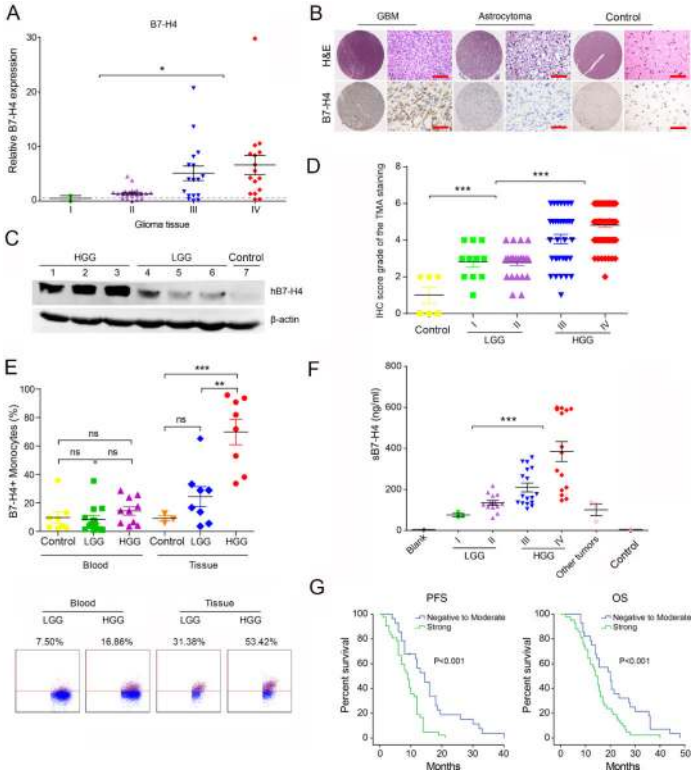

Figure 1. B7-H4 expression on human gliomas

(A) RT-qPCR detection of relative B7-H4 expression in WHO grade I - IV glioma tissues. Differences in mRNA expression in gliomas compared with non-tumor controls (grey line) are shown (n=2/I, 21/II, 17/III, 16/IV, LGG (I+II) compared to HGG (III+IV), * T test, $P < 0.05$). (B) TMA IHC detection of B7-H4 in clinical GBMs, astrocytoma and control (Scale bar: 200μm). (C) WB showing B7-H4 expression in HGG, LGG and Non-Tumor controls. Representative results of at least two independent experiments. (D) Statistics of TMA immunohistochemical detection of B7-H4 in clinical GBMs (n=6/control, 11/I, 22/II, 35/III, 70/IV, control vs LGG (I+II): p<0.001, LGG (I+II) vs HGG (III+IV): $P < 0.001$, t test). (E, top) FACS analysis of B7-H4 expression on fresh Mφs/microglia (CD11b+) isolated from peripheral blood or glioma tissue (n=8/healthy blood for control group, 13/LGG blood group, 10/HGG blood group, 3/non-tumor controls, 8/LGG tissue group, 8/HGG tissue group. T test, NS, no significance. **, $P < 0.01$, ***, $P < 0.001$). (Bottom) Data are representative dot plots of four individuals. (F) Quantification of ELISA-detected human sB7-H4 concentration in CSF from LGG, HGG and other brain disease (CSF: n= 1/blank, 3/I, 13/II, 17/III, 15/IV, 3/others tumors (2 metastatic tumor and 1 meningioma), 1/control (mild brain trauma). LGG (I+II) vs HGG (III+IV): T test, ***, $P<0.001$). Error bars indicate SEM. (G) IHC staining intensity of B7-H4 in tumor niche was evaluated in 70 GBM and used to divide the patients into two groups: negative to moderate expression and strong expression. PFS (left) and OS (right) were then compared between two groups. (Progression-free survival (PFS) and overall survival (OS) after the operation were calculated using the Kaplan–Meier method and analyzed with the log-rank test, $P<0.001$)

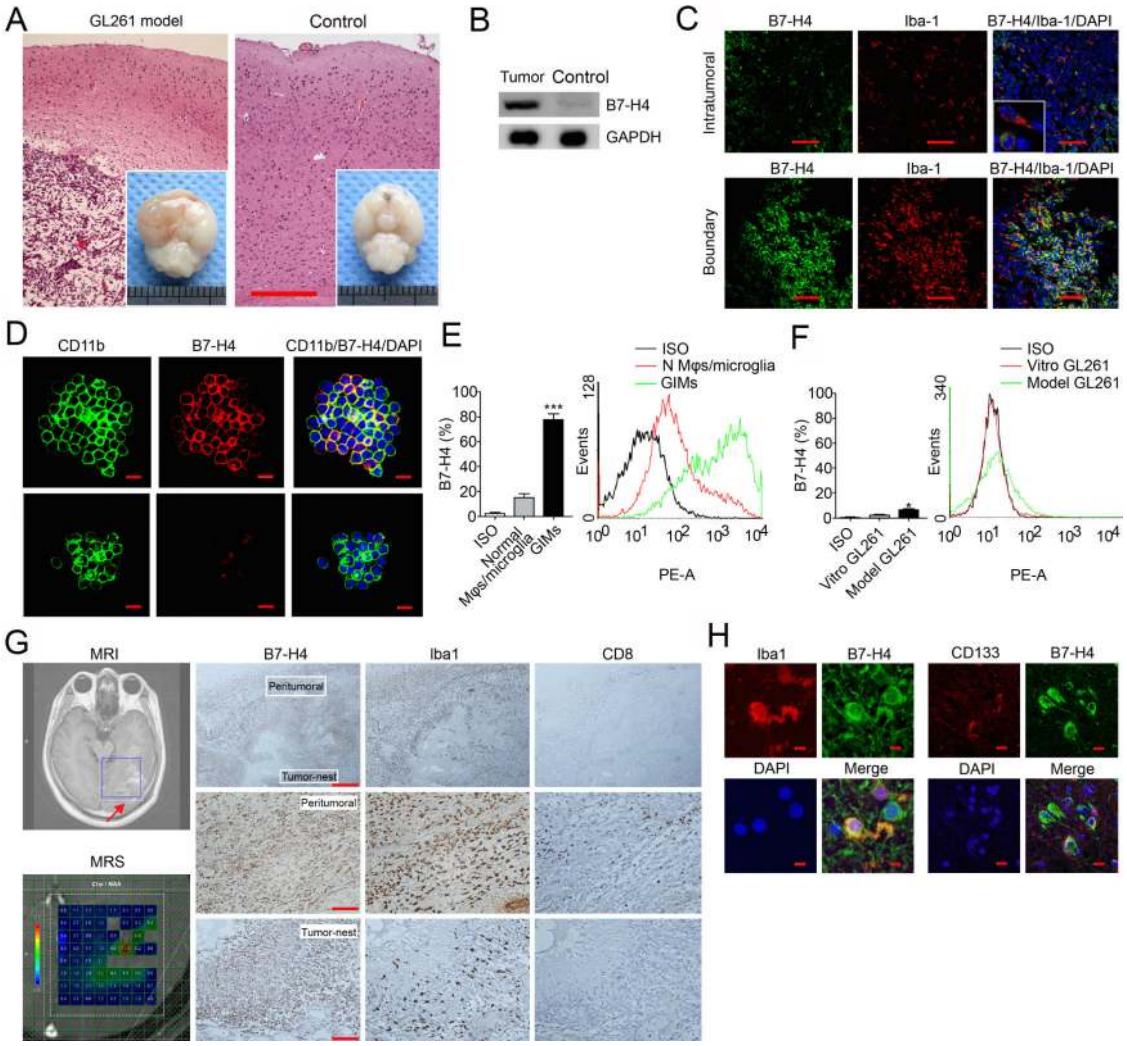

Figure 2. B7-H4 distribution and localization in glioma, GIMs, and CD133+ cells

(**A**) Representative H&E of C57BL/6 mice (20d after intracerebral injection of 1×10^5 GL261 cells per brain). (*Inset*) Glioma shown with macroscopic pictures (left panel). Normal mouse brain images serve as control (right panel). Scale bar: 200μm. (**B**) WB showing B7-H4 expression in tumor tissues compared to Control. (**C)(**Top) IF staining for B7-H4 and Iba-1 (marker of Mϕs/microglia cells) of sections from the intratumoral region. (*Inset*) B7-H4+ /Iba1+ GIMs shown at high magnification. (Bottom). B7-H4+ GIMs prevalent at the glioma boundary. (88.3% for boundary vs 38.8% for intratumoral, T test, ***P<0.001. Scale bar: 20μm.) (**D**) IF of GIMs from the mouse model (top) and normal microglia from non-tumor control (bottom). Scale bars: 10μm. (**E**) Quantification of B7-H4 between normal Mϕs/microglia (n=10) and GIMs (n=10) by FACS (T test, ***, P<0.001). ISO (isotype, n=10) as control. (**F**) Quantification of B7-H4 on *in vitro* cultured GL261 cells (n=10) and *in vivo* model GL261 cells (CD11b-, n=10) (T test, *, P<0.05). (**G**) Representative MRI (top) and MRS (bottom) images of a GBM patient were analyzed. The white and blue boxes indicate the brain regions selected for MRS review. Analysis of B7-H4 expression patterns were correlated with the distribution patterns of GIMs (Iba1+), which

localized mostly to peritumoral, or stromal region (red arrow navigated by enhanced-MRI images). Adjacent sections of paraffin-embedded brain tissue from this patient were also stained with B7-H4, Iba1 and CD8. The middle and bottom panels show the stromal and tumor nest at higher magnification (top scale bar, 200μm, bottom scale bar, 50μm). (**H**) IF of sectioned human GBM tissues revealed localized B7-H4 expression on GIMs (left panel) and CD133+ tumor cells (right panel, scale bar, 20μm).

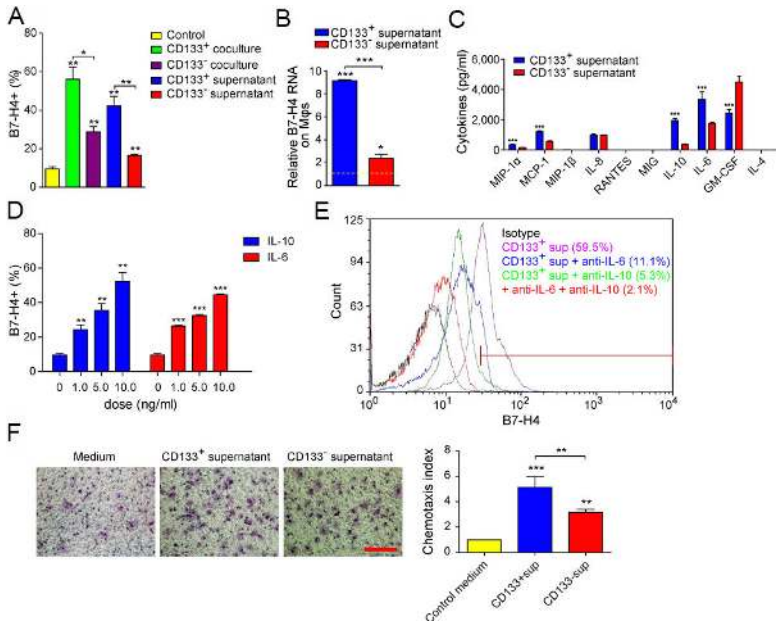

Figure 3. CD133$^+$ cell induce normal human Mφs expression of B7-H4 is mediated by IL-6 and IL-10

(A) Freshly isolated healthy human Mφs were incubated with control medium, CD133+ cells, CD133− cells isolated from human GBM tissue or supernatant from them for 72hr and then analyzed them for B7-H4 expression by FACS (T test, *, $P < 0.05$, **, $P < 0.01$.). (**B**) RT-qPCR for relative B7-H4 gene expression on Mφs cultured in supernatant from either CD133+ or CD133− cells compared with control (yellow line) (**T test,** *, $P < 0.05$, ***, $P < 0.001$). (**C**) Quantity of various cytokines in the supernatant of CD133+ cells or CD133− cells examined by FlowCytomix (T test, ***, $P < 0.001$). (**D**) B7-H4 expression on Mφs was detected by FACS analysis after they were treated with 0, 1.0, 5.0 or 10.0 ng/ml recombinant IL-10 or IL-6 for 72 hr (T test, **, $P < 0.01$, ***, $P < 0.001$). (**E**) Fresh normal Mφs were cultured with supernatant from CD133+ cells for 72 hr in the presence or absence of neutralizing antibodies against IL-6 (500ng/ml) and/or IL-10 (50ng/ml) followed by FACS analysis. (**F**, left) Cell invasion capabilities of normal human peripheral Mφs following culture in either supernatant from CD133+ or CD133− cells, or control medium were analyzed using 6.5mm Transwell with 8.0μm pore polycarbonate membrane insert 24hr later. Scale bar, 100 μm. (right) Quantitative results for chemotaxis index are showed. Data (±SEM) represent 3 independent experiments with similar results. Paired t test, $P<0.01$, ***, $P<0.001$.

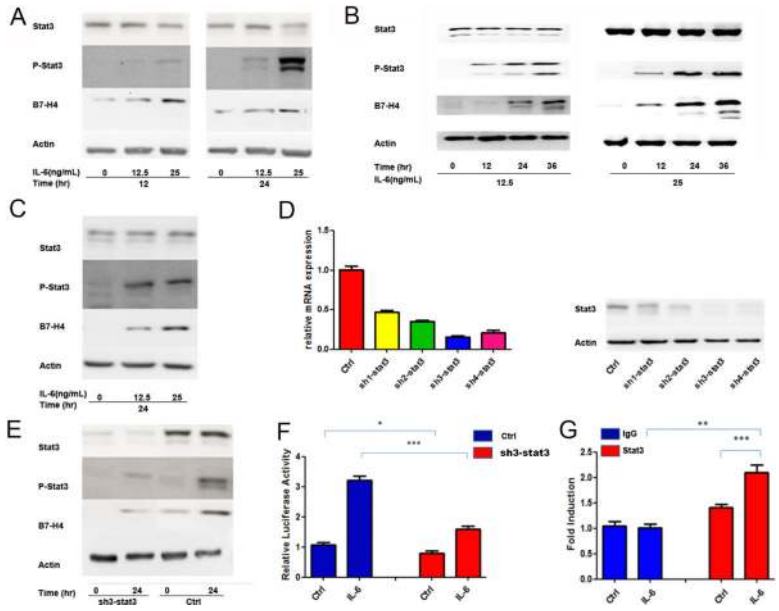

Figure 4. STAT3-dependent B7-H4 expression in microglia/ Mϕs cells

(A) WB analysis of B7-H4 and Stat3 phosphorylation in the mouse BV2 microglia cell line with different time intervals and dose gradient of IL-6. **(B)** Similar finding were reproduced in mouse RAW Mϕs cell line by WB. **(C)** WB analysis of B7-H4 and Stat3 phosphorylation in healthy human peripheral macrophages after incubation for 24 hr with different doses of IL-6. **(D)**Stat3 mRNA expression in the BV2 microglia cells infected with control, shRNA1, shRNA2, shRNA3, and shRNA4. All shRNAs remarkably downregulated Stat3 mRNA (left) and protein levels (right). ShRNA3 was the strongest one, and the other shRNAs had less effect. **(E)** The protein expressions of phosphorylated Stat3 and B7-H4 in BV2 microglia cells infected with shRNA3 or control after being stimulated with IL-6 (25ng/ml). ShRNA3 significantly inhibited phosphorylated Stat3 and B7-H4 protein expression after being stimulated with IL-6. **(F)** BV2 microglia cells were transfected with the above shRNA3 plasmids or control shRNA for 24 hr, and the luciferase activity was measured (T test, *, $P < 0.05$, ***, $P < 0.001$). **(G)** Two Ab (anti-IgG and –STAT3) were used in the ChIP assays using the BV2 microglia cell line treated with or without IL-6 (T test, **, $P < 0.01$, ***, $P < 0.001$).

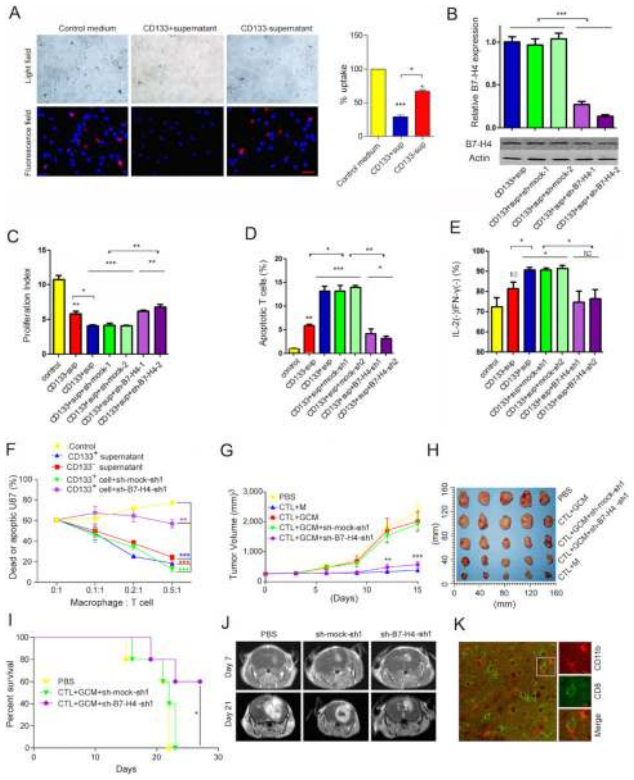

Figure 5. CD133$^+$ cells mediate immunosuppression through B7-H4$^+$ Mϕs in vitro and in vivo

(**A**, left) Normal Mϕs were expanded in either standard medium, supernatant from CD133+ cells, or supernatant from CD133− cells with latex beads (red) before DAPI (blue) staining and phagocytosis assay. Using light and fluorescence microscopy (right, scale bar, 50μm), percentage of cell-mediated uptake (phagocytically active cells/total cells) was determined (Paired t test, *, $P < 0.05$, ***, $P < 0.001$). (**B**) qRT-PCR and WB showed blocking effects of two pairs of sh-B7-H4 and sh-mock lentivirus in CD133+ conditioned Mϕs (T test, *, $P < 0.05$, ***, $P < 0.001$). (**C-F**) Tumor-specific CTLs, activated by U87MG-loaded CD11c+ DCs, were cocultured separately with pretreatment (described above) Mϕ groups, and Mϕ groups in supernatant from CD133+ cells transfected with two pairs of sh-B7-H4 or sh-mock lentivirus. Immunoreactivity, specifically CTL proliferation (**C**, CFSE), apoptosis (**D**, Annexin V/PI staining), and finally IL-2 and IFNγ-expression (**E**) were measured by FACS (T test, *, $P < 0.05$, **, $P < 0.01$, ***, $P < 0.001$). (**F**) Tumor-specific CTLs (CD3+) conditioned with different ratios of pretreated Mϕs (described above) were sorted and cocultured with CFSE-labeled U87MG cells (10:1). U87MG cells were stained with Annexin V/PI to show percentage of apoptosis or death (72hr) (T test, ** $P < 0.05$. *** $P < 0.01$). **(G)** Human U87MG tumors in SCID/NOD mice were measured after injection of 6×10^6 TAA-specific CTLs and different Mϕ preparations (day 12) and excised 15d post-injection (n=5/group) (T test, ** $P < 0.05$. *** $P < 0.01$). **(H)** Tumor size was measured 15d post-injection (n=5/group). (**I**) Intracranial tumor mouse survival was determined following growth/treatment of lesions arising in the right striatum. Treatment entailed intracaudal vein injection (Day 7) of 6×10^6 TAA-specific CTLs and 3×10^6 CD133+cells conditioned Mϕs transfected with (1) sh1-mock (CTL+GCM+sh-mock), (2) sh1-B7-H4 (CTL+GCM+sh-B7-

H4), or (3) PBS (n=5/group). All lesions were characterized by MRI at 7d and 21d (Kaplan-Meier survival analysis, *, $P<0.05$) (**J**) and stained by IF. IF-stained sections show human CD11b+ Mϕs/microglia and human CD8+ T cells colocalizing in three independent experiments (**K**). Scale bars: (left) 20μm, (right) 5μm.

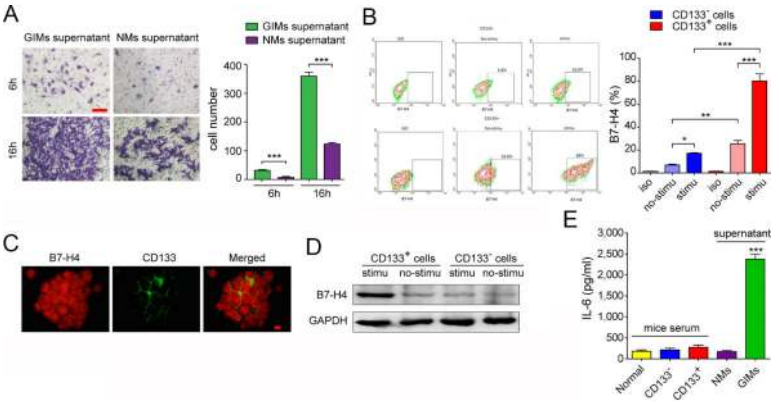

Figure 6. GIMs stimulate CD133+ cell B7-H4 expression and auto-regulation through IL-6

(**A**,left) Serial time points of transwell chemotaxis assay were used to demonstrate the recruitment of GL261 tumor cells in the supernatant of GIMs and normal Mϕs/microglia (NMs). Scale bar: 10μm. (right) Quantification of immigrated GL261 cells. Data are means ± SE of three independent experiments (n =3, t test, ***, $P < 0.001$). (**B**, left) FC showing B7-H4 expression on CD133− cells and CD133+ cells cultured in vitro with supernatant from GIMs. (Right) Quantification of B7-H4 level on CD133− cells and enriched CD133+ cells upon supernatant stimulation (GIMs from 6 enriched CD133+ cells initiated glioma models/group, T test, *, $P<0.05$, **, $P<0.01$, ***, $P<0.001$). ISO (isotype) as control. (**C**) IF staining for stimulated enriched CD133+ cells. Representative images of three independent staining experiments are shown. Scale bar: 20μm. (**D**) Western blot of B7-H4 protein in enriched CD133+ cells and CD133− cells upon GIMs supernatant. (**E**) Quantification of ELISA-detected IL-6 levels in the serum of normal mice, and mice with CD133− cells or enriched CD133+ cells initiated glioma and supernatant from normal Mϕs/microglia as well as GIMs (n=10, t test, ***, $P<0.001$).